

## Article

# Taguchi Robust Design of Phase Transfer Catalytic Hydrolysis of Polyethylene Terephthalate (PET) Waste in Mild Conditions: Application for the Preparation of Metal–Organic Frameworks

Asma Nouira<sup>1,2,3,\*</sup>, Imene Bekri-Abbes<sup>2</sup>, Isabel Pestana Paixão Cansado<sup>4</sup>  and Paulo Alexandre Mira Mourão<sup>4,\*</sup> 

<sup>1</sup> Renewable Energies Chair, Polo da Mitra da Universidade de Évora, Pólo da Mitra, Apartado 94, 7006-554 Évora, Portugal

<sup>2</sup> Laboratory of Composite Materials and Clay Minerals (LMCMA), CNRSM-Technopole Borj Cédria, University of Carthage, BP 73, Soliman 8027, Tunisia; bekrimene@gmail.com

<sup>3</sup> Faculty of Sciences of Tunis, University of Tunis El Manar, Rue de Tolède, Tunis 2092, Tunisia

<sup>4</sup> Departamento de Química e Bioquímica, Escola de Ciências e Tecnologia, MED—Mediterranean Institute for Agriculture, Environment and Development & Change—Global Change and Sustainability Institute, Universidade de Évora, Rua Romão Ramalho n° 59, 7000-671 Évora, Portugal; ippc@uevora.pt

\* Correspondence: asma.nouira@uevora.pt (A.N.); pamm@uevora.pt (P.A.M.M.)

**Abstract:** With the rapid increase in polyethylene terephthalate (PET) usage in recent years, recycling has become indispensable in mitigating environmental damage and safeguarding natural resources. In this context, this study presents a methodology for valorizing PET waste through phase transfer catalytic hydrolysis conducted at a low temperature (80 °C) and atmospheric pressure, with the goal of recovering the terephthalic acid (TPA) monomer. The recovered TPA monomer was subsequently utilized as a precursor for the synthesis of metal–organic frameworks (MOFs). Tributylhexadecyl phosphonium bromide (3Bu6DPB) was selected as the phase transfer catalyst due to its efficiency and sustainability. The process parameters, including the concentration of NaOH, the wt.% of catalyst to PET, and the concentration of PET in the solution, were varied to optimize the hydrolysis reaction. The Taguchi design methodology with an L9 (3<sup>3</sup>) orthogonal array was employed to analyze the influence of these factors on the depolymerization time. The analysis of variance (ANOVA) results revealed that the concentration of NaOH was the most significant factor, contributing to 93.3% of the process efficiency, followed by the wt.% of the catalyst to PET (6.5%). The findings also demonstrated that the concentration of NaOH had the greatest impact ( $\Delta = 4.27$ , rank = 1), while the concentration of PET had the smallest effect ( $\Delta = 0.16$ , rank = 3). The optimal conditions for PET depolymerization were achieved in 75 min with 20 g/100 mL of NaOH, 12 wt.% of catalyst to PET, and 5 g/100 mL of PET. The recovered TPA monomer was further employed as an organic ligand to synthesize Fe(III)-TPA MOFs under mild conditions (80 °C for 24 h). The X-ray diffraction (XRD) analysis revealed the simultaneous formation of MOF-235(Fe) and MIL-101(Fe), two multifunctional materials with diverse properties and applications. This study highlights an efficient approach for producing low-cost MOFs while promoting urban waste recycling, contributing to an integrated strategy for PET recycling and resource valorization.

**Keywords:** PET waste; recycling; depolymerization; terephthalic acid; phase transfer catalyst; metal–organic framework



Academic Editors: Mona Semsarilar and Vincent Ladmiral

Received: 24 November 2024

Revised: 14 February 2025

Accepted: 25 February 2025

Published: 6 March 2025

**Citation:** Nouira, A.; Bekri-Abbes, I.; Cansado, I.P.P.; Mourão, P.A.M.

Taguchi Robust Design of Phase Transfer Catalytic Hydrolysis of Polyethylene Terephthalate (PET) Waste in Mild Conditions:

Application for the Preparation of Metal–Organic Frameworks. *Solids* **2025**, *6*, 10. <https://doi.org/10.3390/solids6010010>

**Copyright:** © 2025 by the authors. Licensee MDPI, Basel, Switzerland.

This article is an open access article distributed under the terms and conditions of the Creative Commons Attribution (CC BY) license (<https://creativecommons.org/licenses/by/4.0/>).

## 1. Introduction

In recent decades have witnessed rapid growth in the plastic industry and a dramatic increase in the number of manufactured plastic products (especially soft drink and water

bottles), which has negatively affected the environment due to the ubiquity of polyethylene terephthalate (PET) waste. Recent statistical studies estimate that plastic packaging constitutes approximately 36% of global plastic productions, with 46% of it either being incinerated or discarded into the environment [1]. To deal with this crisis, it has become crucial to introduce sustainable approaches [1,2]. PET waste can be valorized through various recycling methods, including re-extrusion (primary recycling process), mechanical recycling (secondary process), chemical recycling (tertiary process), and incineration processes (quaternary process) [3–5].

During the chemical recycling by solvolysis, PET waste is depolymerized to monomers or oligomers using different solvents. There are a wide spectrum of solvent/PET possible combinations, including aminolysis (solvent = amines, monomer = terephthalamide derivatives), neutral hydrolysis (solvent = water, monomer = terephthalic acid (TPA)), acidic hydrolysis (solvent = acids, monomer = TPA), hydrolysis (solvent = alkaline solution, monomer = TPA), alcoholysis (solvent = alcohol, monomer = dimethyl terephthalate), and glycolysis (solvent = ethylene glycol, monomer = Bis(2-hydroxyethyl) terephthalate (PHET)) [3–5].

Among all these possibilities, only hydrolysis facilitates the recovery of terephthalic acid (TPA) from PET waste. TPA is an attractive and rigid ligand that is widely utilized in coordination chemistry [5]. More specifically, neutral hydrolysis requires high temperatures and pressures, often resulting in the formation of oligomers [6,7]. Acid hydrolysis, such as that involving sulfuric acid, poses challenges due to its corrosive nature, necessitating the use of costly equipment [8]. Alkaline hydrolysis involves treating PET with a sodium hydroxide (NaOH) solution at elevated pressures and temperatures reaching up to 220 °C [8]. In this process, TPA is recovered as a precipitate by the neutralization of a disodium salt of TPA [9].

To enhance the efficiency and feasibility of the PET hydrolysis process, this study focuses on optimizing alkaline hydrolysis by reducing the amount of NaOH and lowering the reaction temperature. This optimization is achieved through the use of tributylhexadecyl phosphonium bromide as a phase transfer catalyst and Taguchi design to minimize the number of experiments. Research has demonstrated that tributylhexadecylphosphonium bromide is one of the most effective phase transfer catalysts. It enhances the hydrolysis reaction by promoting contact between hydroxide anions and polymer chains [10,11].

Metal–organic frameworks (MOFs) are hybrid organic–inorganic materials with highly organized structures, formed by the coordination of metal ions with organic ligands. By varying these building blocks, materials with diverse properties and applications can be developed (such as water treatment, gas adsorption, catalysis, controlled drug delivery, and luminescence) [12,13]. Among organic ligands, terephthalic acid is widely used in MOF synthesis due to its excellent coordination properties and stability. Furthermore, TPA can be recovered from PET waste, and several MOFs based on TPA derived from PET waste have been successfully synthesized [14–18]. For example, MOF-235, Fe(III)-TPA-based MOF, is an environmentally friendly material with applications across various domains. It was first synthesized by the Yaghi group in 2005 using a solvothermal method [19]. The chemical formula of MOF-235 is  $[\text{Fe}_3\text{O}(\text{1,4-BDC})_3(\text{DMF})_3][\text{FeCl}_4]$  (where 1,4-BDC represents TPA and DMF refers to N,N-dimethylformamide). The material forms octahedral crystals in which each trivalent iron atom is surrounded by TPA molecules, resulting in an overall cationic framework with a +1 charge per formula unit. This positive charge is balanced by  $\text{FeCl}_4^-$  ions, which are localized within different cavities, as illustrated in Figure 1.

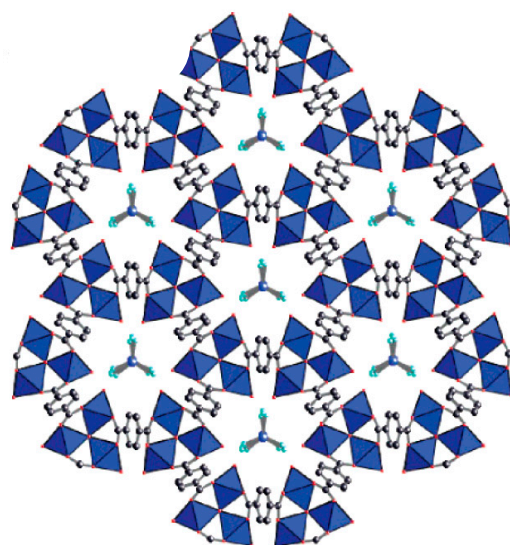


**Figure 1.** Chemical structure of MOF-235 (Fe—blue; O—red; Cl—teal; C—gray) [19].

While numerous MOF structures have been synthesized and investigated, to the best of our knowledge, TPA derived from PET waste has not been utilized in previous studies to prepare MOF-235. To enhance and optimize the recovery of TPA from PET waste for use as an organic linker in MOF materials, this study aims to depolymerize PET under milder conditions compared to those previously reported. The process optimization is achieved through the use of an efficient catalyst and the application of a Taguchi robust design, reducing operating costs and making the process more economical at lower temperatures and atmospheric pressures. In this study, the alkaline hydrolysis of PET waste was examined at 80 °C using a 12–20 g/100 mL of NaOH solution, with 3Bu6DPB phosphonium salt serving as a phase transfer catalyst. The recovered monomer (TPA) was subsequently utilized as a ligand in the synthesis of MOF materials.

## 2. Materials and Methods

### 2.1. Materials

All the chemicals were of analytical grade. Tributylhexadecyl phosphonium bromide (3Bu6DPB) and sodium hydroxide pellets (NaOH) were purchased from Novachim, Co., Ltd, Marseille, France and HCl from Sharlau, Co., Ltd, Barcelone, Spain. On the other hand,  $\text{FeCl}_3 \cdot 6\text{H}_2\text{O}$  was obtained from Oxford Lab Fine Chem, Co., Ltd, Maharashtra, India and N,N-dimethylformamide (DMF, 99%) and 98%  $\text{H}_2\text{SO}_4$  were obtained from Fluka, Switzerland.

### 2.2. Taguchi Optimization of Depolymerisation of PET Waste

#### 2.2.1. Taguchi Methodology

The Taguchi method is a statistical approach to experimental design that uses orthogonal arrays to evaluate process parameters, assess their performance, and analyze their impact on the overall process. Its distinct advantage over other models lies in its ability to assess performance and robustness while minimizing the number of experimental trials. This makes it a cost-effective and efficient tool for optimization studies [20]. The ratio of the signal (desired performance) to the standard deviation (noise), denoted as the *S/N ratio*, is a key performance introduced by Taguchi. It measures the robustness of a process against variations. The signal represents the desired value or performance characteristic, while the noise encompasses variations or uncontrollable factors that may cause deviations from the desired outcome. A higher *S/N ratio* indicates that the desired performance is stronger

relative to variations, reflecting a more stable and robust process. Depending on the nature of the problem or the response variable to be optimized, Taguchi utilizes three types of *S/N ratios* (Equations (1)–(3)):

Larger-the-better: Used when attempting to maximize the response:

$$s/Nratio = -10 \times \log_{10} \left( \frac{1}{n} \sum_{i=1}^n \left( \frac{1}{y_i} \right) \right) \quad (1)$$

Smaller-the-better: Used when attempting to minimize the response:

$$s/Nratio = -10 \times \log_{10} \left( \frac{1}{n} \sum_{i=1}^n (y_i^2) \right) \quad (2)$$

Nominal-the-best: Used when attempting to make the response attain a specific value (*T*):

$$s/Nratio = -10 \times \log_{10} \left( \frac{1}{n} \sum_{i=1}^n ((y_i - T)^2) \right) \quad (3)$$

where  $y_i$  is the individual observed value and  $n$  is the number of trials. The selection of an appropriate Signal-to-Noise (*S/N*) ratio in Taguchi methods is guided by the specific objective of the experiment, which is classified into three distinct categories: smaller-is-better, larger-is-better, and nominal-is-best. Each category employs a unique *S/N ratio* formulation to address the problem requirements. The overarching objective of the Taguchi design approach is to identify the optimal parameter settings that maximize the *S/N ratio*. By doing so, the process achieves enhanced performance and robustness, effectively reducing the influence of variability and noise factors [20].

### 2.2.2. Taguchi Optimization of PET Depolymerization by Catalytic Hydrolysis

Prior to the experiments, PET water bottles were collected, and their caps and labels were removed. The bottles were subsequently washed with water and detergent to remove impurities and then dried in an oven at 40 °C for 4 h. Once dried, the bottles were cut into sections approximately 3 × 3 to 5 × 5 mm<sup>2</sup> in size. In the experiments, three factors were evaluated using the Taguchi method with an L9 (3<sup>3</sup>) orthogonal array, implemented through Minitab Statistical Software 22. As presented in Table 1, the study examined three factors: the weight percentage (wt.%) of the catalyst to PET, the concentration of NaOH, and the concentration of PET in the solution. Each of these process parameters was evaluated at three levels (L) to systematically analyze their influence. The performance parameter considered was the time required for PET to totally depolymerize (in minutes). The optimization of performance parameters and the calculation of the signal-to-noise (*S/N*) ratio were performed for each experiment, and the smaller-the-better criterion was selected, aligning with the Taguchi approach. The software (MINITAB) identifies nine significant experimental runs, reducing the total from the 27 runs (3<sup>3</sup> = 27) that would be required for three reaction parameters, each with three levels.

**Table 1.** The key operating factors and their levels;

Factors	Units	Levels		
		Level 1	Level 2	Level 3
Concentration of NaOH	g/100 mL	12	15	20
Concentration of PET	g/100 mL	5	10	15
Wt.% of catalyst/ PET	%	3	7	12

Table 2 presents the experimental conditions for PET hydrolysis, including variations in the NaOH concentration, PET amount, and catalyst percentage. Different combinations

of these parameters were tested to optimize the PET hydrolysis conditions and minimize the depolymerization time. According to run n°1, 5 g of PET waste and 0.15 g of the catalyst (3Bu6DPB) were added to 100 mL of 7 g/L of NaOH solution, and the mixture was stirred continuously at 80 °C in a 250 mL Pyrex round-bottom flask equipped with a reflux condenser. The reaction was considered complete when all PET flakes were fully dissolved. The depolymerization time was recorded for each experiment. Afterward, the reaction solution was neutralized to pH = 7 using H<sub>2</sub>SO<sub>4</sub> and filtered to remove additives and colorants. Subsequently, the solution was acidified to pH = 2 to facilitate the precipitation of terephthalic acid. The precipitated TPA was purified by washing with an excess of water and then dried at 378 K. Tributylhexadecyl phosphonium bromide is soluble in water, which facilitates its removal through a simple water washing step. To recover the catalyst from the washing water, its significantly higher solubility in methanol compared to water can be utilized. This is achieved through a methanol/water extraction process where the washing water is mixed with methanol to dissolve the catalyst, followed by separation of the organic phase. The tributylhexadecyl phosphonium bromide is then recovered by evaporating the methanol under reduced pressure, leaving behind the phosphonium salt.

**Table 2.** The L<sub>9</sub> OA design of experiment for catalytic hydrolysis of PET waste (the green color corresponds to the optimal combination with the highest S/N value).

Run	Concentration of NaOH	Concentration of PET	Wt% Catalyst to PET	Depolymerization Time (min)	S/N ratio
1	12	5	3	135	−42.61
2	12	10	7	130	−42.29
3	12	15	12	125	−41.94
4	15	5	7	115	−41.21
5	15	10	12	105	−40.42
6	15	15	3	120	−41.58
7	20	5	12	75	−37.50
8	20	10	3	88	−38.89
9	20	15	7	82	−38.28

### 2.3. Synthesis of MOF-235 by the Hydrothermal Route Using Recovered TPA

MOF-235 was synthesized as described in the literature, with slight modifications [19]. Briefly, a 1:1 molar ratio of the previously obtained TPA and FeCl<sub>3</sub>·6H<sub>2</sub>O were dissolved in 10 mL of N,N-dimethylformamide (DMF). The solution was stirred until homogeneous. The clear reaction solution was then transferred into a Teflon-lined autoclave and heated at 80 °C for 24 h. Orange crystals of MOF-235 were recovered by filtration, washed with DMF and distilled water, and then dried at 60 °C for 12 h.

### 2.4. MOF-235 Characterizations

X-ray diffraction (XRD) spectra were obtained using an X'Pert Pro Panalytical X-ray diffractometer and a D8 ADVANCE system from Bruker, San Jose, USA. The diffractograms were processed with X'Pert High Score Plus 4.0 software and were performed with a resolution of 0.02° and 30 scans. Fourier Transform Infrared (FTIR) spectroscopy was recorded with 64 scans at a resolution of 4 cm<sup>−1</sup>. The functional groups of TPA and MOF were identified using the ATR-FTIR spectroscopy technique within the range of 400–4000 cm<sup>−1</sup>. The analysis was conducted with a Perkin Elmer Spectrum instrument, a two-beam IR spectrophotometer equipped with an Attenuated Total Reflection accessory. Scanning Electron Microscopy (SEM) images of the selected samples were captured using a Quanta 650 FEG scanning electron microscope, FEI Co Ltd, Oregon, US with a resolution range from 30× to 200,000×, and an accelerating voltage varying between 0.2 and 30 kV.

The coupled Differential Thermal Analysis/Thermogravimetric (DTA/TG) curves were recorded using a Setsys Evolution 1750 SETARAM instrument KEP Technologies, Sophia Antipolis France, coupled with a thermo-balance. The sample was carefully weighed and heated to 500 °C at a rate of 20 °C per minute under a nitrogen atmosphere.

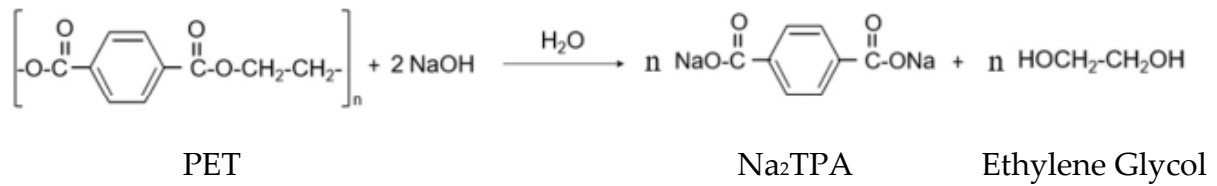
### 3. Results and Discussion

#### 3.1. Catalytic Depolymerization Mechanism

During the first step of the alkaline hydrolysis of PET (Figure 2, Step I), hydroxide ions act as nucleophilic centers, attacking the electrophilic carbonyl carbon (C=O) of the ester groups in PET chains. This reaction produces disodium terephthalate ( $\text{Na}_2\text{TPA}$ ) and ethylene glycol (EG). In the second step of the process (Figure 2, Step II), sulfuric acid is added to the disodium terephthalate solution until the pH reaches 2–3, resulting in the precipitation of terephthalic acid (TPA) [21]. It is important to note that the excess sulfuric acid also leads to the formation of sodium sulfate ( $\text{Na}_2\text{SO}_4$ ). Consequently, the precipitated TPA was washed with deionized water to remove any impurities. The catalytic alkaline hydrolysis of PET using a phase transfer catalyst (PTC) is an efficient method that enhances the depolymerization process by facilitating the transfer of hydroxide ions from the aqueous alkaline phase to the organic solid phase of PET. Quaternary ammonium and phosphonium salts are commonly employed as phase transfer catalysts due to their ability to promote the migration of reactants between phases. They contain a positively charged cation, enabling them to attract and solvate hydroxide anions ( $\text{OH}^-$ ), thereby allowing the anions to cross the phase boundary between the aqueous and organic PET phases. Once in the organic phase, the  $\text{OH}^-$  anions can attack the carbonyl (C=O) groups of PET. While numerous studies have examined the role of ammonium in PET depolymerization, relatively little attention has been given to phosphonium salts [21]. In this study, tributylhexadecyl phosphonium bromide (3Bu6DPB) was selected due to its high efficiency as a phase transfer catalyst. As illustrated in Figure 3, the catalytic reaction using 3Bu6DPB involves transferring hydroxide ions ( $\text{OH}^-$ ) from the aqueous phase into the organic phase where the PET polymer is located. This transfer occurs through the formation of an ion pair complex between the  $\text{OH}^-$  anion and the phosphonium cation (PTC– $\text{OH}^-$  complex), making the  $\text{OH}^-$  anions more lipophilic. This property allows the PTC– $\text{OH}^-$  complex to migrate from the aqueous phase into the organic PET phase. Reference [11] provided a detailed analysis of several ammonium and phosphonium salts as phase transfer catalysts for the alkaline hydrolysis of PET waste.

These catalysts differ in regard to water solubility, alkyl group composition, and anion nature. The study showed that the high reactivity of 3Bu6DPB salts is attributed to their strong compatibility with the organic phase and to the efficient anion transfer. This efficiency is facilitated by the highly lipophilic cation and the presence of large alkyl groups, which ensure significant partitioning of the cation–anion pair into the organic phase.

### Step I



### Step II

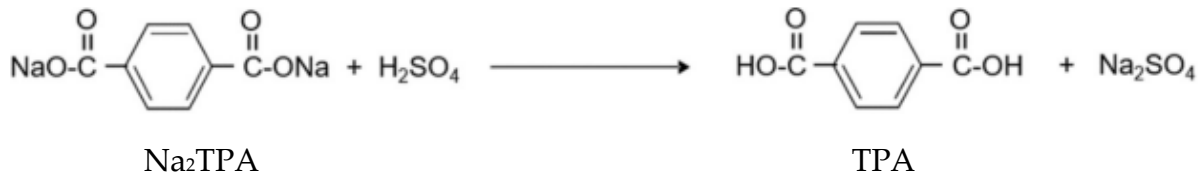


Figure 2. NaOH Alkaline hydrolysis reaction of PET waste.

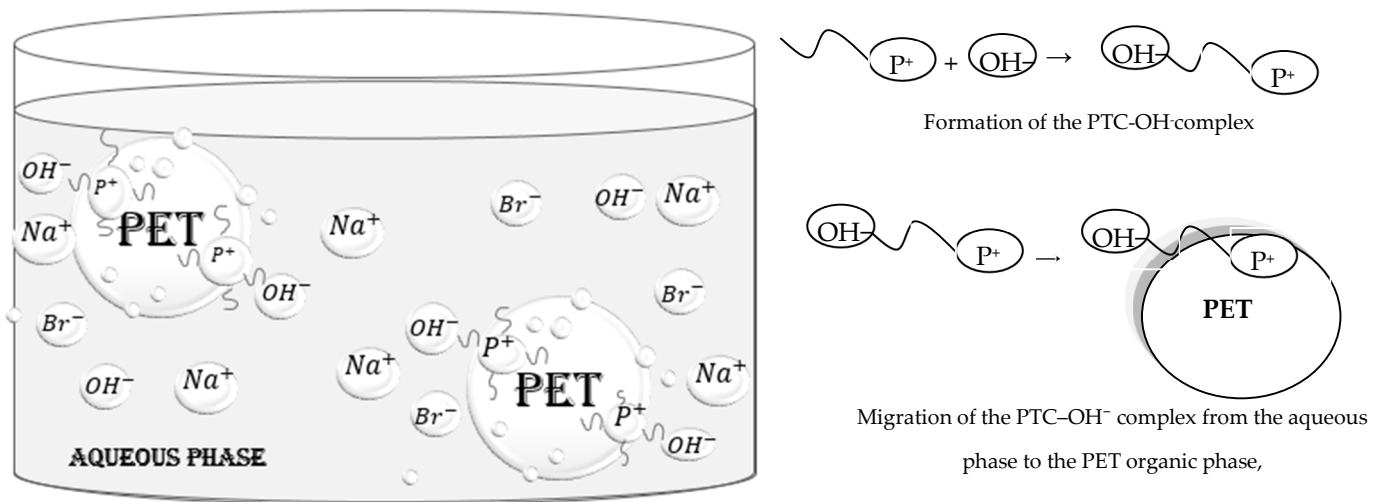


Figure 3. Mechanism of the PTC catalytic alkaline hydrolysis of PET.

### 3.2. Taguchi Optimization Regression and ANOVA Study

The optimization of the parameters of depolymerization, using the Taguchi method and ANOVA, enabled the complete depolymerization of PET at 80 °C and atmospheric pressure in the shortest time possible. Table 3 presents the *S/N ratio* and the mean response for each factor and each level, including the delta value, which represents the difference between the maximum and minimum *S/N* values for each factor. The calculation method involves subtracting the *S/N ratio* of the minimum level from the *S/N ratio* of the maximum level for each factor [22]. The ranks of the different factors are determined based on delta values: rank 1 is assigned to the factor with the highest delta value, rank 2 to the second-highest, and so on. The results presented in Table 3 show that the concentration of NaOH has the greatest influence on both the *S/N ratio* and the mean response for the depolymerization time. The wt.% of catalyst to PET has the second greatest influence, followed by the concentration of PET.

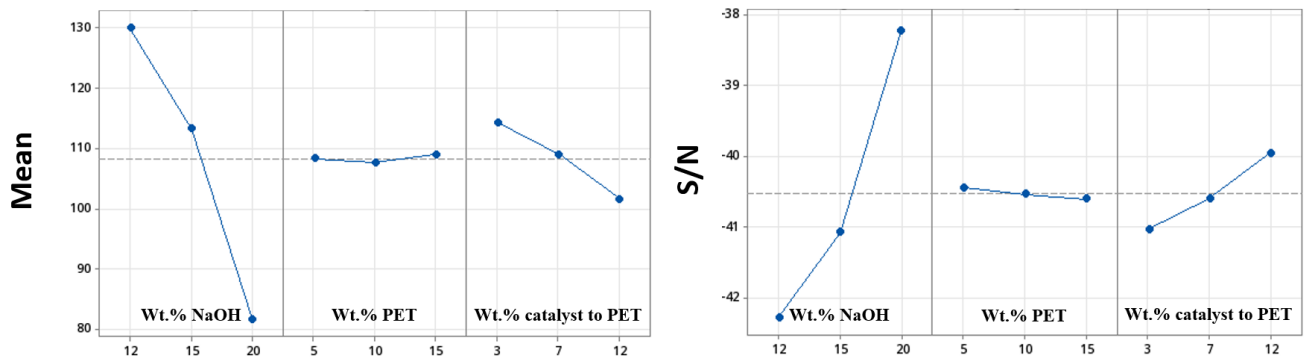
**Table 3.** The *S/N* and mean values at each level; the delta and rank of each factor.

<b>S/N</b>			
<b>Level</b>	<b>Concentration of NaOH (g/100 mL)</b>	<b>Concentration of PET (g/100 mL)</b>	<b>Wt.% Catalyst to PET</b>
1	−42.27	−40.44	−41.03
2	−41.07	−40.53	−40.59
3	−38.0	−40.60	−39.95
Delta	4.27	0.16	1.08
Rank	1	3	2
Optimum	Level 3	Level 2	Level 1
<b>Mean</b>			
<b>Level</b>	<b>Concentration of NaOH (g/100 mL)</b>	<b>Concentration of PET (g/100 mL)</b>	<b>Wt.% Catalyst to PET</b>
1	130	108	114
2	113.33	113.33	109
3	81.67	109	101.67
Delta	48.33	5.33	12.33
Rank	1	3	2

Based on these findings, the optimal levels for maximizing the *S/N ratio* are level 3 for the concentration of NaOH (20 g/100 mL), level 1 for the concentration of PET (5 g/100 mL), and level 3 for the wt.% of catalyst to PET (12%). Further confirmation of the significance of these parameters can be found in the slopes of the *S/N* vs. parameters plots (Figure 4). The quasi horizontal line in the plot indicates that the corresponding parameter has a slight effect on the response [21]. These results suggest that the concentration of PET has a slight effect on the depolymerization time, particularly within the variation range of concentration of NaOH between 12% and 20%.

Figure 5a–e illustrates the 3D surface plots of various process parameters. Specifically, Figure 5a,b show the effect of the concentration of PET and NaOH on the depolymerization time. It is evident that, as the concentration of PET increases, the depolymerization time also increases. This trend is expected, as higher PET concentrations reduce the contact area available for the alkaline solution, which hinders the diffusion of hydroxide ions ( $\text{OH}^-$ ) into the interior of the PET particles, thereby slowing the reaction [22]. Additionally, at lower PET concentrations, increasing the NaOH concentration initially decreases the reaction time, suggesting an acceleration of the process. However, at higher PET concentrations, this effect becomes less pronounced. Figure 5c,d illustrate the effect of the concentration of NaOH and the catalyst-to-PET on the depolymerization time. The plots indicate that, as the NaOH concentration increases, the reaction time decreases, evidenced by the downward slope of the surface plot. The influence of the catalyst-to-PET ratio on the reaction time is less significant compared to NaOH concentration. Figure 5e,f reveal a wave-like structure with peaks and valleys, indicating that certain combinations of the wt.% of the catalyst and PET result in shorter or longer process times. Additionally, Taguchi 3D surface plots provide a visual tool to estimate the optimal combination of factors by identifying the region where the response variable is at its lowest level. From the 3D plots and Table 4, the ranges of factors to minimize the process time can be estimated as follows: concentration

of NaOH concentrations in the range of 19–20%, wt.% catalyst/PET of 5–12 wt.%, and the concentration of PET between 4.5 and 13%.



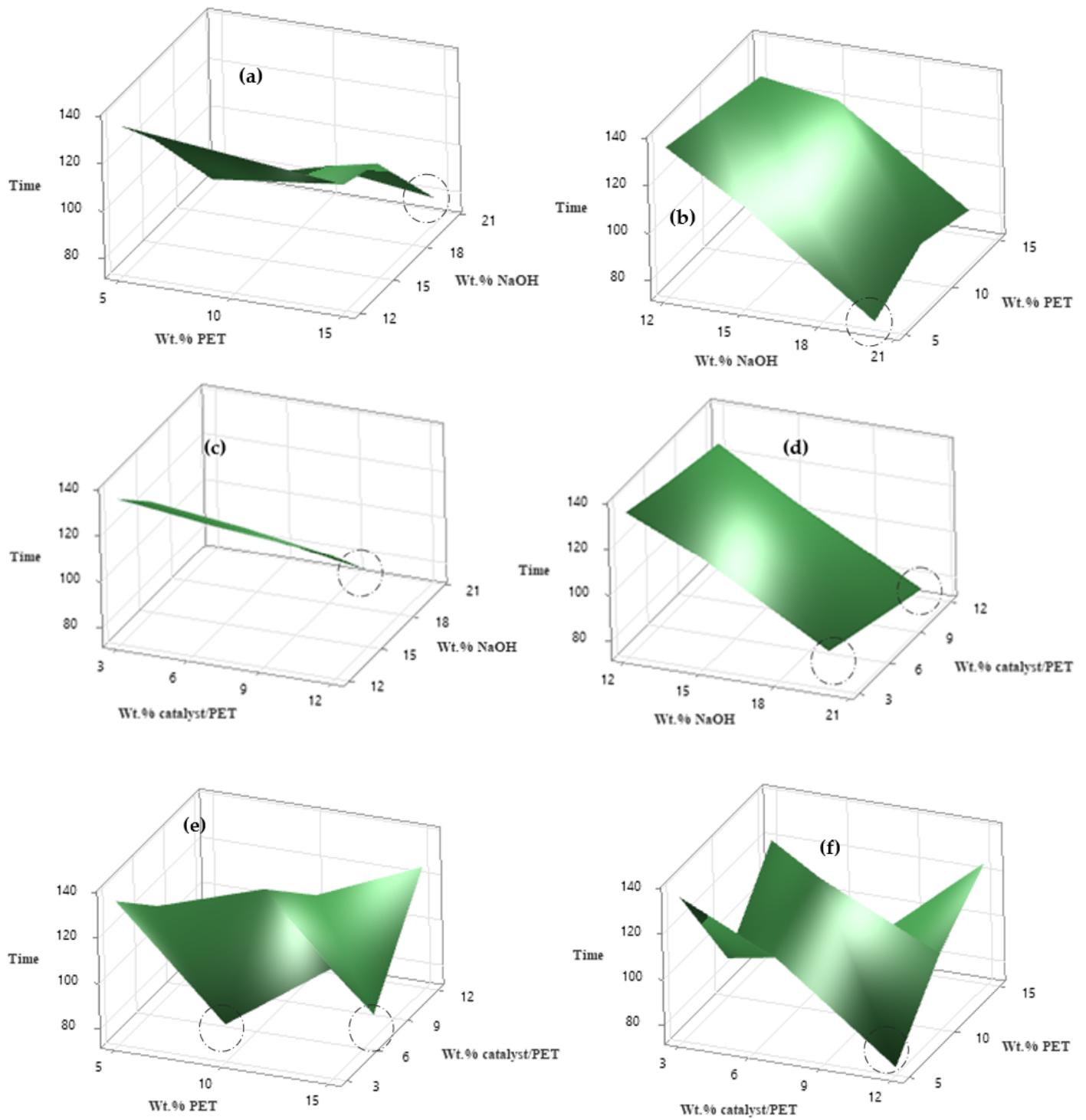
**Figure 4.** Graph of mean of depolymerization time of PET flakes and  $S/N$  response for different factors.

Figure 6a,c illustrate the effect of the interaction between the concentration of NaOH and that of PET on the depolymerization process time. They show that, regardless of whether the PET flake loading is low or high, increasing the concentration of NaOH reduces the depolymerization time. Similarly, Figure 6b,e highlight the interaction between the percentage of catalyst and NaOH. As expected, for all NaOH concentrations, the depolymerization time decreases with an increase in catalyst concentration. For instance, at 20% NaOH, PET flakes are completely depolymerized in approximately 1.5 h with 5% of catalyst to PET. This time further reduces to about 1 h when the catalyst percentage increases to 15%. These results align well with findings reported in previous studies [10,11].

Based on Supporting Information (S1), which presents the ANOVA results for the  $S/N$  ratios obtained for PET depolymerization time, it is evident that the concentration of NaOH and the wt.% of catalyst to PET have  $p$ -values less than 0.05 (0.02 for concentration of NaOH and 0.024 for wt.% catalyst to PET). This indicates that these factors are statistically significant at the 0.05 level of significance. Additionally, these two factors exhibit the largest SS Adj values, further confirming their statistical relevance. Conversely, the PET percentage factor has no significant effect, as indicated by its  $p$ -value of 0.692 [22]. This conclusion is further supported by the Pareto chart presented in the Supporting Information, which highlights that NaOH concentration and the catalyst/PET percentage ratio are statistically significant at the 0.05 level of significance.

**Table 4.** Optimal PET depolymerization values based on factor variation (different optimized values have been deduced from circle zones in Figure 5a–f).

Figure Factor	Figure 5a	Figure 5b	Figure 5c	Figure 5d	Figure 5e	Figure 5f
Concentration of PET	4.5	5.75	5.5	-	8–13	5.5
Concentration of NaOH	20	20	20	19	-	-
Wt% catalyst to PET	-	-	-	5–12	11	11.5



**Figure 5.** Three-dimensional surface plot of the combination of process parameters (optimized zones are marked by circles).

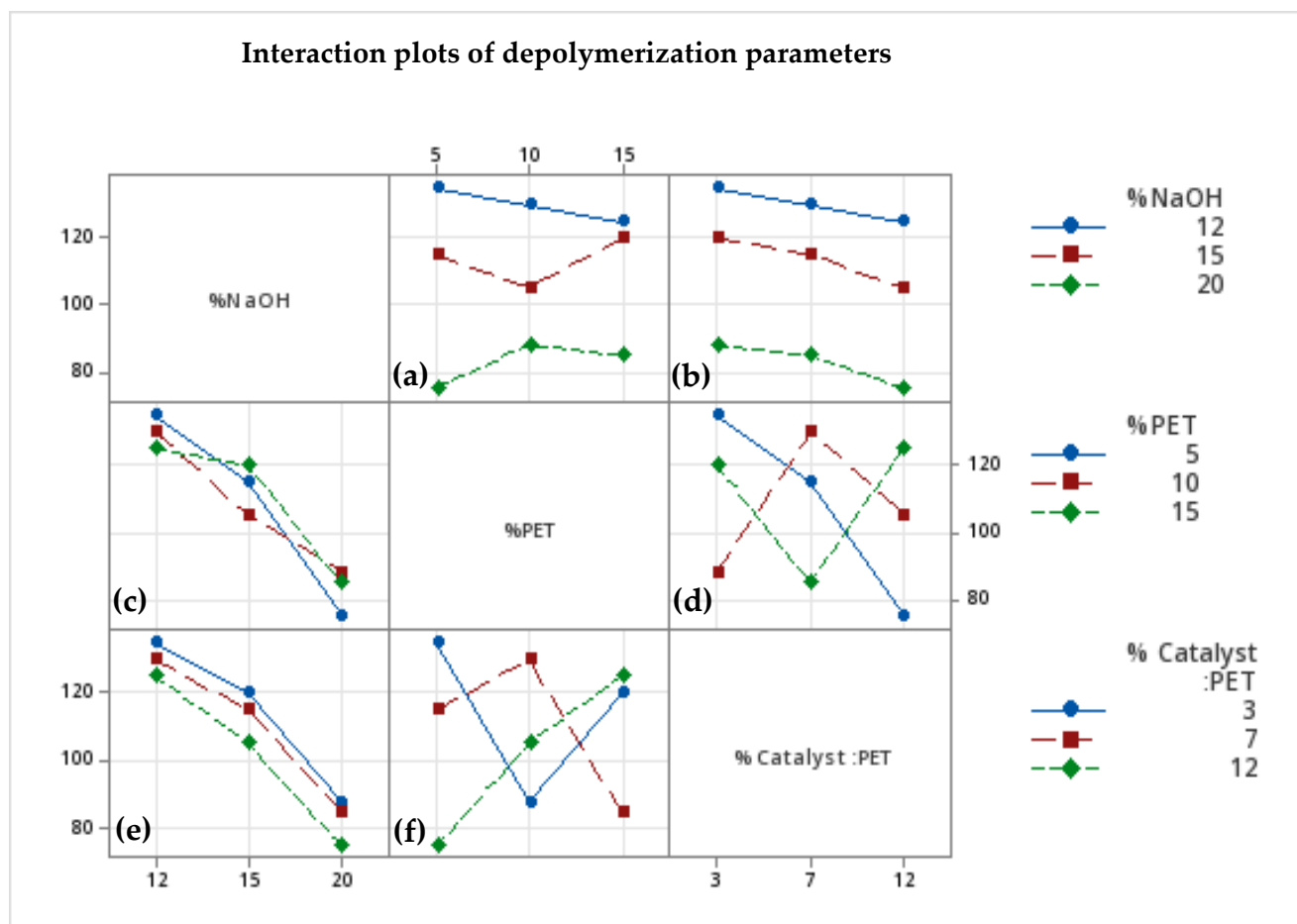


**Figure 6.** Interaction plots of different parameters and the depolymerization time of PET. (a) Interaction of the concentration of NaOH versus that of PET; (b) interaction of the concentration of NaOH versus wt.% catalyst to PET; (c) interaction of the concentration of NaOH versus that PET; (d) interaction of the concentration of PET versus wt.% catalyst to PET; (e) interaction of the concentration of NaOH versus that of PET; and (f) interaction of the concentration PET versus wt.% catalyst to PET.

### 3.3. Characterization of the Recuperated TPA

#### 3.3.1. FT-IR Analysis

The spectrum of the recovered TPA is shown in Figure 7. It revealed characteristic peaks corresponding to the functional groups of terephthalic acid. Specifically, the C=O stretch ( $3000\text{--}2500\text{ cm}^{-1}$ ), C=C stretch ( $1675\text{ cm}^{-1}$ ), C–C aromatic stretch ( $1427\text{ cm}^{-1}$ ), and C–O stretch ( $1237\text{ cm}^{-1}$ ) were observed in the sample obtained from the depolymerization of PET. Additionally, bands at  $1014\text{ cm}^{-1}$ ,  $1089\text{ cm}^{-1}$ , and  $1237\text{ cm}^{-1}$  are attributed to the bending vibrations of CO groups. These findings align well with reference data, confirming the presence of TPA [23].

#### 3.3.2. X-Ray Diffraction

The X-ray diffractograms of the TPA obtained through the depolymerisation of PET is presented in Figure 8. The XRD pattern of the TPA powder displayed peaks at  $2\theta$  values of  $17.12^\circ$  (110),  $25.1^\circ$  (222),  $27.4^\circ$  (220),  $30.9^\circ$  (121),  $39.6^\circ$  (212), and  $41^\circ$  (222). The corresponding  $2\theta$  values are consistent with the reported values [23].

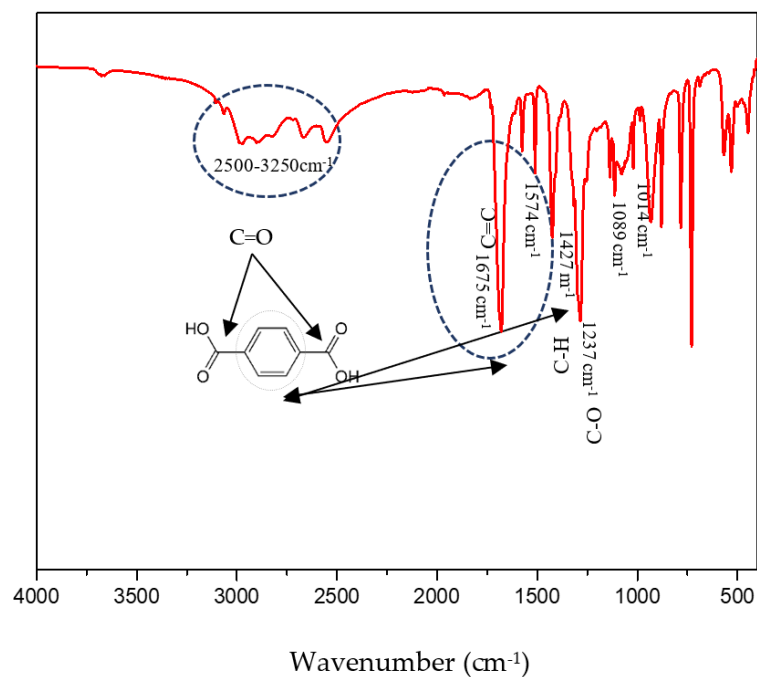


Figure 7. FTIR Spectrum of recovered TPA.

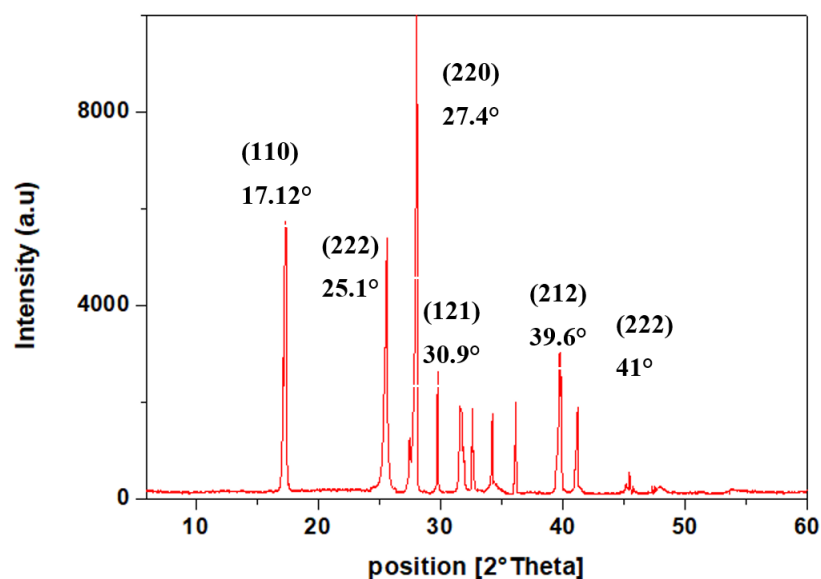


Figure 8. X-ray diffractogram of recovered TPA.

### 3.3.3. Thermal Characteristics of TPA

The TPA recovered from the hydrolysis of PET waste was subjected to Differential Thermal Analysis/Thermogravimetric (DTA/TG) analyses to evaluate its thermal decomposition profile. The results of these analyses are shown in Figure 9. A significant mass loss of approximately 70% occurred in the temperature range of 350–430 °C, which can be attributed to the decomposition of the ester groups into volatile products. According to the literature [23–25], the carboxylic acid groups undergo thermal decomposition within this temperature range.

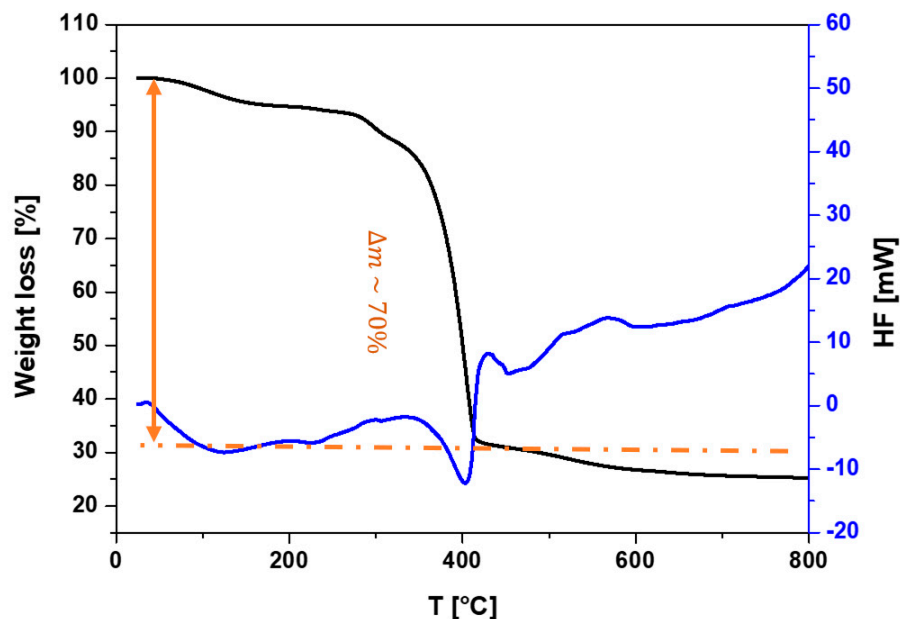


Figure 9. DTA/TG thermograms of recovered TPA.

### 3.4. Application of the Recuperated TPA Used as Ligand to Prepare MOF-235

The TPA recovered from the depolymerization of PET was used as an organic linker for the preparation of MOF-235. The surface chemical composition of MOF-235 was characterized using Fourier Transform Infrared (FTIR-ATR) spectroscopy, as shown in Figure 10. The FTIR spectrum revealed some characteristics bands, including those at  $823\text{ cm}^{-1}$  and  $1012\text{ cm}^{-1}$ , which were attributed to C-H vibrations of the aromatic ring.

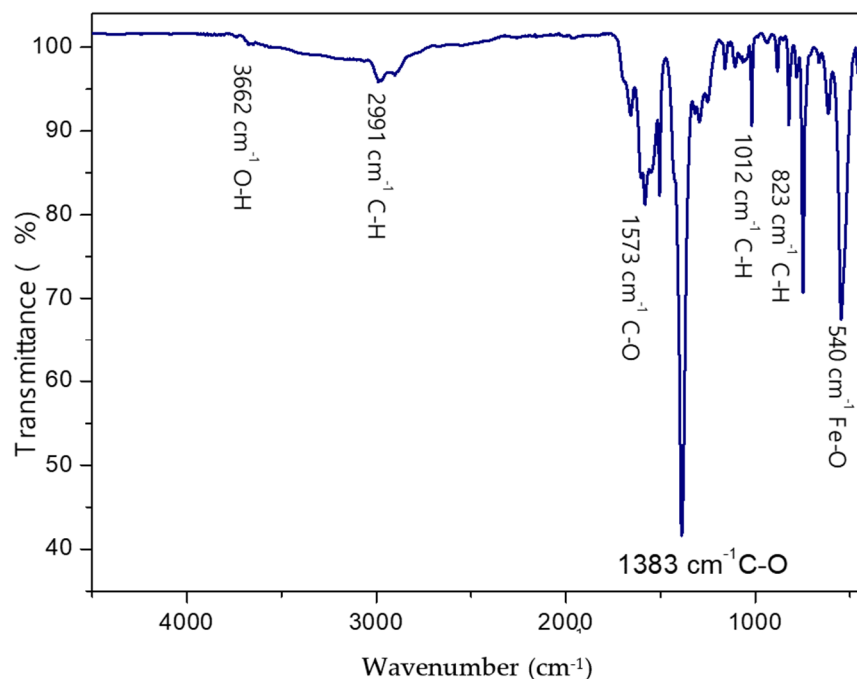


Figure 10. Infrared spectrum of synthesized MOF.

Additionally, the bands at  $1573\text{ cm}^{-1}$  and  $1383\text{ cm}^{-1}$  corresponded to the asymmetric and symmetric stretching vibrations of the C-O bonds in carboxyl groups. The broad band observed around  $3400\text{ cm}^{-1}$  was assigned to the stretching vibrations of O-H groups. Furthermore, the peak of Fe-O in Fe-MOFs appears at  $550\text{ cm}^{-1}$ . The low-intensity band at

2991  $\text{cm}^{-1}$  is related to the C-H vibrations of DMF. These findings are in good agreement with previous data [26,27].

### 3.4.1. X-Ray Diffraction

The X-ray diffraction (XRD) pattern of the prepared MOF powder is presented in Figure 11. The XRD peaks corresponding to the MOF-235 structure are observed at  $2\theta = 10.27^\circ$ ,  $13^\circ$ ,  $17^\circ$ ,  $22.0^\circ$ , and  $27.5^\circ$  which are in good agreement with the previously reported literature [27,28]. Additionally, the appearance of additional peaks at  $2\theta = 9.52^\circ$ ,  $11^\circ$ ,  $18.22^\circ$ ,  $22.0^\circ$ , and  $27.5^\circ$  can be observed, corresponding to another Fe-TPA MOF, namely MIL-101(Fe), as reported in reference [29]. MIL-101(Fe) is a well-known iron(III) terephthalate MOF with the molecular formula  $[\text{Fe}_3\text{O}(\text{OH})(\text{H}_2\text{O})_2(1,4\text{-BDC})_3]$ , where 1,4-BDC represents 1,4-benzenedicarboxylate (TPA). MOF-235 and MIL-101 exhibit distinct differences in their morphologies and pore structures. MIL-101 features a three-dimensional porous structure consisting of two differently sized nanocages with diameters of 29 Å and 34 Å, connected by windows with diameters of 12 Å and 16 Å. In contrast, MOF-235 has a one-dimensional hexagonal channel structure with a diameter of 6.7 Å<sup>2</sup> [30]. Simonsson et al. [30] conducted a detailed study on the synthesis of MIL-101 and MOF-235, as well as their simultaneous formation. Their findings indicated that a synthesis process at 80 °C for 24 h did not yield a pure MOF-235 phase. Instead, additional peaks corresponding to MIL-101 were detected in the XRD spectrum, confirming the co-formation of both frameworks under these conditions. Various adjustments were tested to optimize the synthesis process, including using anhydrous solvents, employing freshly purchased chemicals, repeating the synthesis multiple times, conducting thermal treatments in different types of vessels, and varying the drying temperature. However, none of these modifications yielded a significant improvement. It was found that a higher DMF proportion and lower synthesis temperature appear to favor MOF-235 formation. Conversely, using a non-insulated vessel, such as a glass bottle, tends to promote the formation of MIL-101, which is the more thermodynamically stable phase [30].

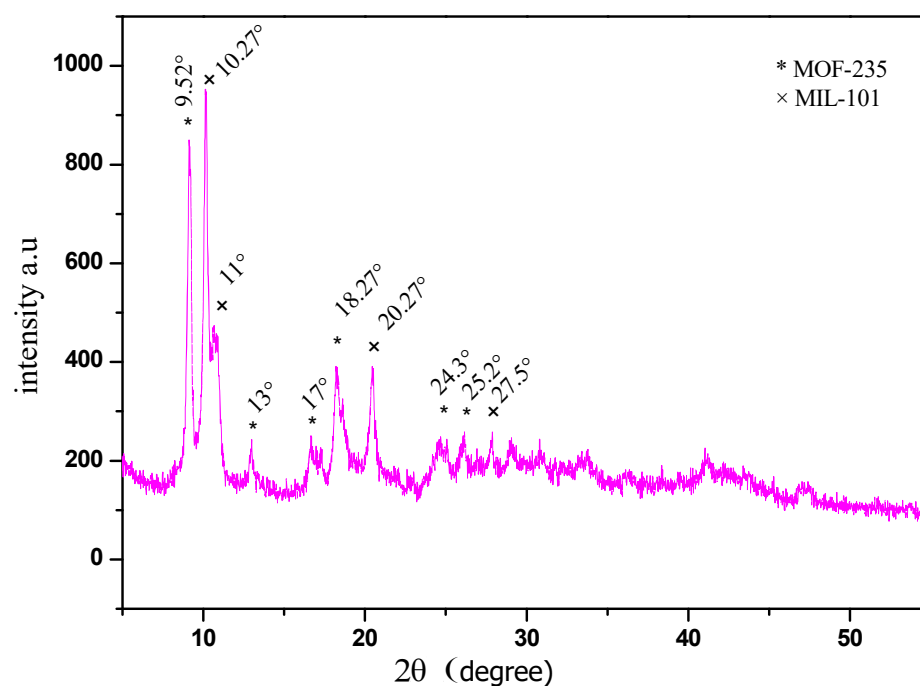
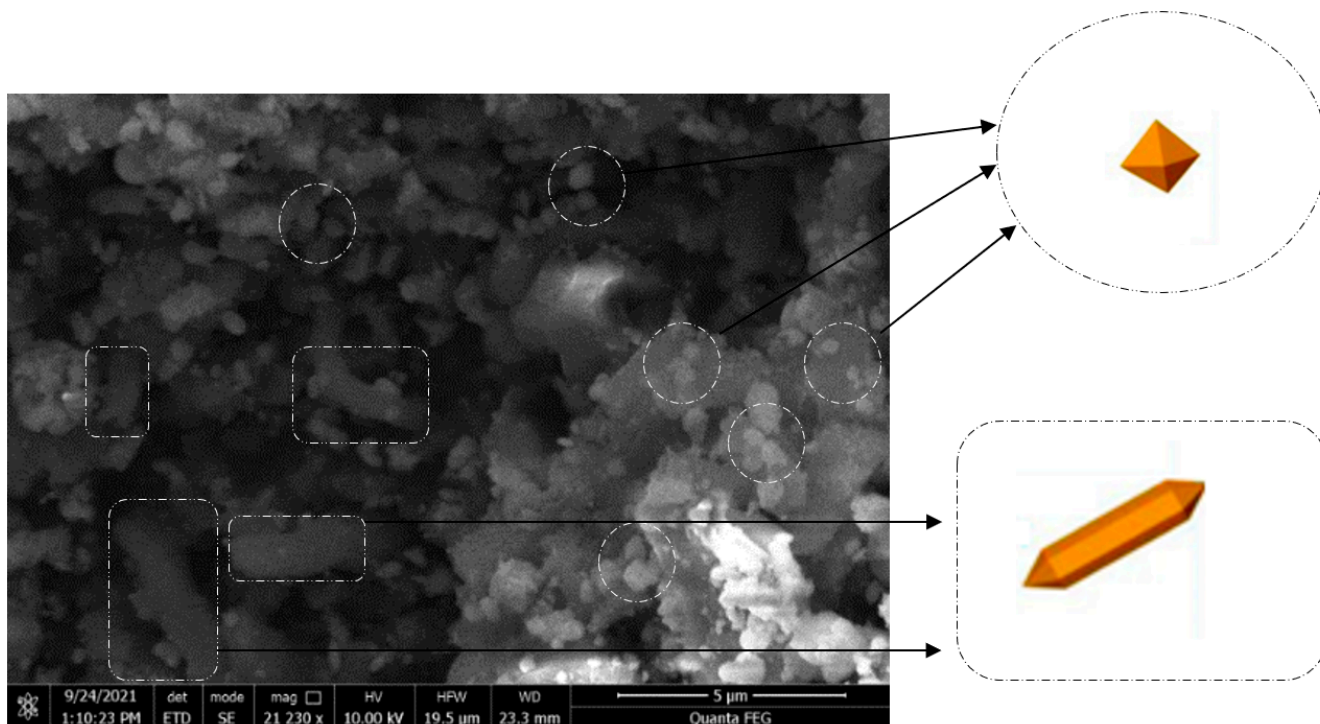


Figure 11. X-ray diffractogram of synthesized MOF-235 (\*) associated with MIL-101 (x).

### 3.4.2. SEM Morphology

An SEM analysis was performed to characterize the micromorphology of the prepared MOF, as shown in Figure 12. The analysis revealed the presence of two distinct micromorphologies. Hexagonal bipyramidal structures, with particle sizes ranging from 150 nm to 0.5  $\mu\text{m}$ , were associated with the MOF-235 structure [31].



**Figure 12.** SEM image and EDS of prepared MOF.

Additionally, it is possible to observe the presence of tubular and spindle-like morphologies, with an average length of 3–5  $\mu\text{m}$  and a diameter of approximately 1  $\mu\text{m}$ , which were attributed to the MIL-101 structure [32].

## 4. Conclusions

This study explored the alkaline hydrolysis depolymerization of PET bottle waste using an efficient phase transfer catalyst, tributylhexadecyl phosphonium bromide. The depolymerization reaction was conducted under mild conditions, specifically under lower atmospheric pressures and at temperatures not exceeding 80  $^{\circ}\text{C}$ . Optimization parameters, including the wt.% of catalyst/PET, the concentration PET, and the concentration of NaOH, were investigated using the Taguchi robust design method. The optimal conditions yielding the highest signal-to-noise (S/N) ratios and the shortest depolymerization time (75 mn) were 20% NaOH (level 3,  $S/N = -38.22$ ), 5% of PET (level 1,  $S/N = -40.44$ ), and 12 wt.% catalyst/PET (level 3,  $S/N = -39.95$ ). The results demonstrated that the  $p$ -values for the concentration of NaOH and the wt.% of catalyst/PET were less than  $\alpha = 0.05$ , indicating that these factors were statistically significant. The 3D plot of interaction of different factors reveals that the time of depolymerization for PET is primarily influenced by the concentration of NaOH and that the impact wt.% of catalyst/PET is less significant. Characterization techniques, including FTIR, XRD, and TGA, confirmed that TPA was recovered using this process. Furthermore, it was successfully utilized as an organic linker to synthesize iron-based porous metal–organic frameworks, specifically MOF-235 and MIL-101. These findings suggest that catalytic depolymerization is a promising and

sustainable approach for converting PET waste into valuable TPA, which can serve as a precursor for the production of advanced metal–organic framework materials.

**Supplementary Materials:** The following supporting information can be downloaded at <https://www.mdpi.com/article/10.3390/solids6010010/s1>: Figure S1: Pareto chart of different factors  $\alpha = 0.05$ ; Table S1: ANOVA results of the *S/N ratios* obtained for the observed PET conversion time.

**Author Contributions:** A.N. and I.B.-A. participated in methodology development, experimentation, data collection and analysis, and writing of the paper. I.P.P.C. and P.A.M.M. contribute in data analysis, optimization, edit and review the manuscript. All authors have read and agreed to the published version of the manuscript.

**Funding:** This work was supported by the Tunisian Ministry of Higher Education and Scientific Research.

**Data Availability Statement:** The data used on this study are available from the corresponding authors on reasonable request.

**Acknowledgments:** The authors gratefully acknowledge the Tunisian Ministry of Higher Education and Scientific Research and MED—Mediterranean Institute for Agriculture, Environment and Development and Change—Global Change and Sustainability Institute and Departamento de Química e Bioquímica, Escola de Ciências e Tecnologia, Universidade de Évora.

**Conflicts of Interest:** The authors declared no conflicts of interest.

## References

1. Worm, B.; Lotze, H.K.; Jubinville, I.; Wilcox, C.; Jambeck, J. Plastic as a persistent marine pollutant. *Annu. Rev. Environ. Resour.* **2017**, *42*, 1–26. [[CrossRef](#)]
2. Noura, A.; Bekri-Abbes, I.; Srasra, E.; Cansado, I.; Mourão, P. Valorisation of plastic waste from the beverage industry through its transformation into adsorbent and solid fuel materials. *Comptes Rendus. Chim.* **2022**, *26*, 77–93. [[CrossRef](#)]
3. Allaf, A.W.; Al Lafi, A.G.; Alzier, A.; Ajaya, R.; Mougrabiya, M.A.; Ali, A.A.; Adriby, S. A study on microwave-assisted chemical recycling of polyethylene terephthalate (PET) waste. *J. Polym. Res.* **2024**, *31*, 41. [[CrossRef](#)]
4. Lechuga-Islas, V.D.; Sánchez-Cerrillo, D.M.; Stumpf, M.; Guerrero-Santos, S.R.; Schubert, U.S.; Guerrero-Sánchez, C. Thermo-responsive polymer catalysts for polyester recycling processes: Switching from homogeneous catalysis to heterogeneous separations. *Polym. Chem.* **2023**, *14*, 1893–1904. [[CrossRef](#)]
5. Abedsoltan, H. A focused review on recycling and hydrolysis techniques of polyethylene terephthalate. *Polym. Eng. Sci.* **2023**, *63*, 2651–2674. [[CrossRef](#)]
6. Güçlü, G.; Yalçinyuva, T.; Özgümüş, S.; Orbay, M. Simultaneous glycolysis and hydrolysis of polyethylene terephthalate and characterization of products by differential scanning calorimetry. *Polymer* **2003**, *44*, 7609–7616. [[CrossRef](#)]
7. Rosen, B.I. Preparation of Purified Terephthalic Acid from Waste Polyethylene Terephthalate. U.S. Patent 5,095,145, 10 March 1992.
8. Aguado, J.; Serrano, D. *Recycling of Plastic Wastes*; University of York: York, UK, 1999.
9. Nikolaevich, L.; Vladimirovna, I.; Zulfatovich, M. Method for Waste Pet Alkaline Hydrolysis with Terephthalic Acid Production. RU Patent RU2616299C1, 14 April 2017.
10. Kosmidis, V.A.; Achilias, D.S.; Karayannidis, G.P. Poly (ethylene terephthalate) recycling and recovery of pure terephthalic acid. Kinetics of a phase transfer catalyzed alkaline hydrolysis. *Macromol. Mater. Eng.* **2001**, *286*, 640–647. [[CrossRef](#)]
11. López-Fonseca, R.; González-Marcos, M.P.; González-Velasco, J.R.; Gutiérrez-Ortiz, J.I. Chemical recycling of PET by alkaline hydrolysis in the presence of quaternary phosphonium and ammonium salts as phase transfer catalysts. *WIT Trans. Ecol. Environ.* **2008**, *109*, 511–520. [[CrossRef](#)]
12. Chen, J.; Ma, J.; Fan, Q.; Zhang, W.; Guo, R. A sustainable chrome-free tanning approach based on Zr-MOFs functionalized with different metals through post-synthetic modification. *Chem. Eng. J.* **2023**, *474*, 145453. [[CrossRef](#)]
13. Chen, J.; Ma, J.; Fan, Q.; Zhang, W. An eco-friendly metal-less tanning process: Zr-based metal-organic frameworks as novel chrome-free tanning agent. *J. Clean. Prod.* **2023**, *382*, 135263. [[CrossRef](#)]
14. Manousi, N.; Zachariadis, G.; Deliyanni, E.; Samanidou, V. Applications of metal-organic frameworks in food sample preparation. *Molecules* **2018**, *23*, 2896. [[CrossRef](#)] [[PubMed](#)]
15. Giliopoulos, D.; Zamboulis, A.; Giannakoudakis, D.; Bikiaris, D.; Triantafyllidis, K. Polymer/Metal Organic Framework (MOF) Nanocomposites for biomedical applications. *Molecules* **2020**, *25*, 185. [[CrossRef](#)] [[PubMed](#)]
16. Kampouraki, Z.; Giannakoudakis, D.; Nair, V.; Hosseini-Bandegharai, A.; Colmenares, J.; Deliyanni, E. Metal organic frameworks as desulfurization adsorbents of dbt and 4,6-dmdbt from fuels. *Molecules* **2019**, *24*, 4525. [[CrossRef](#)]

17. Boukayouht, K.; Bazzi, L.; Daouli, A.; Maurin, G.; Hankari, S.E. Ultrarapid and sustainable synthesis of trimetallic-based mof (crnife-mof) from stainless steel and disodium terephthalate-derived PET wastes. *ACS Appl. Mater. Interfaces* **2024**, *16*, 2497–2508. [[CrossRef](#)] [[PubMed](#)]
18. Zhang, F.; Chen, S.; Nie, S.; Luo, J.; Lin, S.; Wang, Y.; Yang, H. Waste PET as a reactant for lanthanide MOF synthesis and application in sensing of picric acid. *Polymers* **2019**, *11*, 2015. [[CrossRef](#)]
19. Sudik, A.C.; Côté, A.P.; Yaghi, O.M. Metal-organic frameworks based on trigonal prismatic building blocks and the new “acs” topology. *Inorg. Chem.* **2005**, *44*, 2998–3000. [[CrossRef](#)]
20. Unal, R.; Dean, E.B. Taguchi approach to design optimization for quality and cost: An overview. In Proceedings of the 1991 Annual Conference of the International Society of Parametric Analysts, NASA Langley Research Center, Hampton, VA, USA, 1 January 1991.
21. Barredo, A.; Asueta, A.; Amundarain, I.; Leivar, J.; Miguel-Fernández, R.; Arnaiz, S.; Epelde, E.; Lopez-Fonseca, R.; Gutierrez-Ortiz, I. Chemical recycling of monolayer PET tray waste by alkaline hydrolysis. *J. Environ. Chem. Eng.* **2023**, *11*, 109823. [[CrossRef](#)]
22. Tseng, K.H.; Shiao, Y.F.; Chang, R.F.; Yeh, Y.T. Optimization of microwave-based heating of cellulosic biomass using Taguchi method. *Materials* **2013**, *6*, 3404–3419. [[CrossRef](#)]
23. Ravichandran, S.A.; Rajan, V.P.; Aravind, P.V.; Seenivasan, A.; Prakash, D.G.; Ramakrishnan, K. Characterization of Terephthalic Acid Monomer Recycled from Post-Consumer PET Polymer Bottles. *Macromol. Symp.* **2016**, *361*, 30–33. [[CrossRef](#)]
24. Chinglenthoba, C.; Mahadevan, G.; Zuo, J.; Prathyumnann, T.; Valiyaveetil, S. Conversion of PET Bottle Waste into a Terephthalic Acid-Based Metal-Organic Framework for Removing Plastic Nanoparticles from Water. *Nanomaterials* **2024**, *14*, 257. [[CrossRef](#)]
25. Kimyonok, A.B.E.; Ulutürk, M. Determination of the Thermal Decomposition Products of Terephthalic Acid by Using Curie-Point Pyrolyzer. *J. Energetic Mater.* **2016**, *34*, 113–122. [[CrossRef](#)]
26. Salem, K.; Zarif, B.R.; Hosseini, F.; Karami, C. Iron terephthalate metal-organic framework (MOF-235) modified with zinc as an efficient adsorbent for removal of tetracycline from aqueous solution. *Desalination Water Treat.* **2024**, *318*, 100393. [[CrossRef](#)]
27. Ge, J.; Wu, Z.; Huang, X.C.; Ding, M. An Effective Microwave-Assisted Synthesis of MOF235 with Excellent Adsorption of Acid Chrome Blue. *J. Nanomater.* **2019**, *2019*, 4035075. [[CrossRef](#)]
28. Li, Y.; Hou, G.; Yang, J.; Xie, J.; Yuan, X.; Yang, H.; Wang, M. Facile synthesis of MOF 235 and its superior photocatalytic capability under visible light irradiation. *RSC Adv.* **2016**, *6*, 16395–16403. [[CrossRef](#)]
29. Huang, Y.; Lin, H.; Zhang, Y. Synthesis of MIL-101(Fe)/SiO<sub>2</sub> composites with improved catalytic activity for reduction of nitroaromatic compounds. *J. Solid State Chem.* **2020**, *283*, 121150. [[CrossRef](#)]
30. Simonsson, I.; Gärdhagen, P.; Andrén, M.; Tam, P.L.; Abbas, Z. Experimental investigations into the irregular synthesis of iron(III) terephthalate metal-organic frameworks MOF-235 and MIL-101. *Dalton Trans.* **2021**, *50*, 4976–4985. [[CrossRef](#)]

31. Deng, Q.; Luo, Z.; Liu, H.; Zhou, Y.; Zhou, C.; Yang, R.; Wang, L.; Yan, Y.; Xu, Y. Facile synthesis of Fe-based metal-organic framework and graphene composite as an anode material for K-ion batteries. *Ionics* **2020**, *26*, 5565–5573. [[CrossRef](#)]
32. Villarroel-Rocha, D.; García-Carvajal, C.; Amaya-Roncancio, S.; Villarroel-Rocha, J.; Torres-Ceron, D.A.; Restrepo-Parra, E.; Sapag, K. MIL-101(Fe)@ceramic-monolith for arsenic removal in aqueous solutions. *Sci. Rep.* **2024**, *14*, 29622. [[CrossRef](#)]

**Disclaimer/Publisher's Note:** The statements, opinions and data contained in all publications are solely those of the individual author(s) and contributor(s) and not of MDPI and/or the editor(s). MDPI and/or the editor(s) disclaim responsibility for any injury to people or property resulting from any ideas, methods, instructions or products referred to in the content.